

Module 3: Velocity Measurement

Lecture 12: Introduction to PIV

The Lecture Contains:

- ☰ Particle image velocimetry
- ☰ Apparatus and Instrumentation
- ☰ Experimental Setup
 - Test Cell
- ☰ Particle Image Velocimetry
 - Seeding Arrangement for PIV
 - Particle Dynamics
 - Generating a Light Sheet
 - Synchronizer

◀ Previous Next ▶

Module 3: Velocity Measurement

Lecture 11:

Particle image velocimetry

The method relies on the fact that small particles introduced in a fluid stream would move with the local fluid velocity. These particles, ideally, are neutrally buoyant with respect to the fluid medium and would not respond to buoyancy forces. This is particularly true for particles of very small diameters where surface forces (that scale with the square of the particle diameter) are much larger than body forces (that scale as diameter cube).

The basic measurements in particle image velocimetry (PIV) relate particle displacement δ over a time period Δt in such a way that velocity is measured as the ratio of displacement and the time interval. The former being a vector, velocity components in the plane of illumination are jointly determined.

Since particle sizes are very small, a small interrogation area selected by the camera for determination for velocity would have several particles. These, in turn, are indistinguishable. The displacement measured is a statistical quantity, applicable for the collection of particles as a whole. The local velocity thus obtained is a *group* velocity of these particles. Statistical methods preferred are usually based on cross-correlation between a pair of images that are separated by a time interval of Δt . Clearly, smaller the time interval, better is the time estimate of velocity. Intervals as small as a few hundred nanoseconds are possible with pulsed lasers; conventional light sources severely fail in this regard. It should also be clear that the cameras used for imaging should record two images of the particle positions separated on the time axis by such a small interval.

The important components of a PIV system would then be (a) a pulsed light source, (b) an imaging system synchronized with the laser, (c) seeding arrangement for creating particles, and (d) software for calculating the cross-correlation function between the image pairs.

The details of a simple PIV system are presented the following sections.



Module 3: Velocity Measurement

Lecture 11:

Apparatus and Instrumentation

A setup for conducting experiments where wake properties of a square cylinder can be studied has been constructed in the laboratory. The setup resembles a low speed wind tunnel, though smaller in the overall size. It is a vertical test cell made of Plexiglas with two optical windows, one for laser sheet and the other for recording images by the CCD camera. The working fluid is air and the direction of overall fluid motion is in the vertically upward direction. Particle Image Velocimetry (PIV) and Hotwire Anemometry (HWA) have been primarily used for velocity measurements. Flow visualization study has been carried out at low seeding density in the PIV setup. The cylinder is oscillated with the help of an electromagnetic actuator. This module describes details of the experimental hardware, including instruments and auxiliary equipment used in the present study. The validation results for proper PIV technique implementation, flow parallelism and turbulence intensity of the test cell and the effect of end plates have been discussed.

 **Previous** **Next** 

Experimental Setup

A schematic drawing of the experimental setup is shown in Figure 3.8. It comprises the following components: flow circuit, traversing mechanism for hotwire measurements, laser (pulsed), CCD camera, seeding arrangement for PIV measurements, and data acquisition system. The free-stream velocity approaching the cylinder has been determined using a pitot-static tube connected to a micro-manometer. The micro-manometer has a resolution of 0.001 mm of H_2O it translates to an error in Reynolds number of about ± 2 . The details of the test cell are discussed here and the PIV and HWA techniques are presented in the following section.

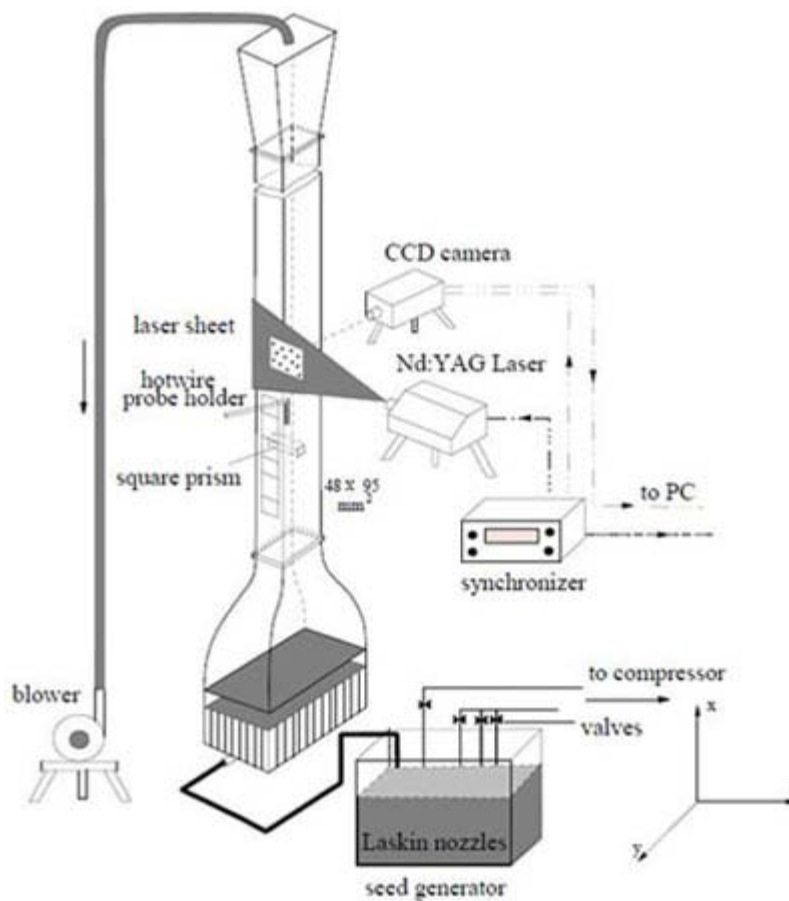


Fig 3.8: Schematic of the experimental setup

Test cell

Experiments have been performed in a vertical open-loop airflow system. The crosssection of the active portion of the test cell (to be called the test section) is $9.5 \times 4.8 \text{ cm}^2$ with an overall length of 2 m. The active length of the test section where wake measurements have been carried out is 0.3 m. A contraction ratio of 10:1 ahead of the test section has been used. Prisms of square cross-section (3-4 mm edge) have been used for experiments as square cylinders. They are made either of Plexiglas or brass and carefully machined for sharp edges. Each cylinder is mounted horizontally with its axis perpendicular to the flow direction. It is supported along the two side walls for fixed cylinder experiments and mounted on actuators for oscillating cylinder experiments.

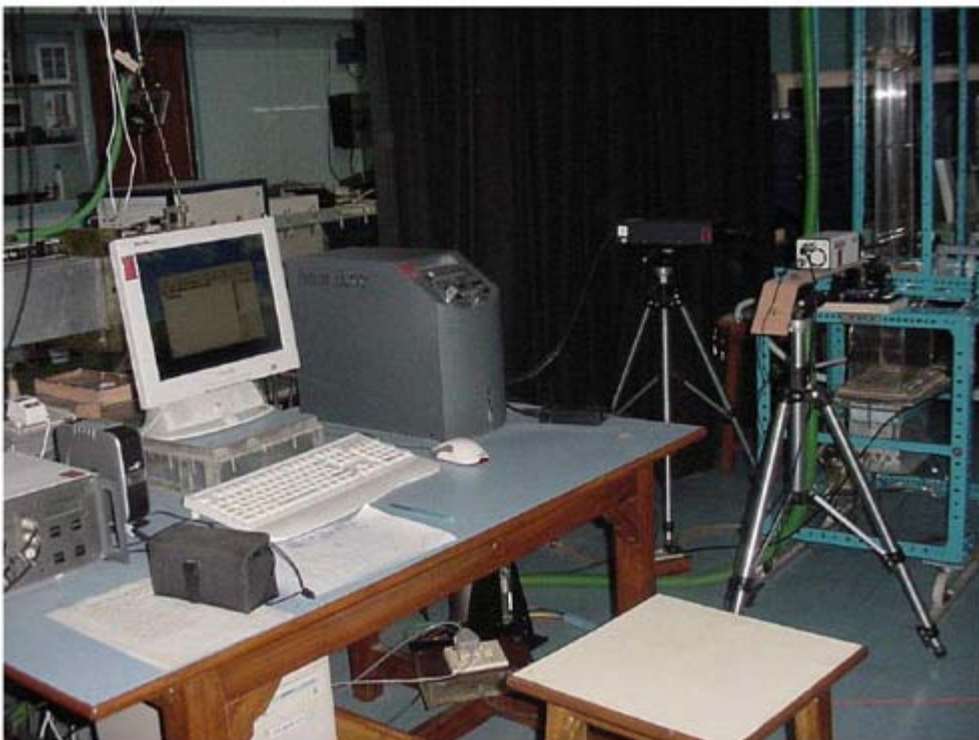


Fig 3.9: Picture of the PIV setup used for the present experiments

Two different L/D ratios (also called aspect ratios) of 16 and 28 have been utilized in the experiments. The two aspect ratios were realized depending on the alignment of the cylinder axis with respect to test section. The corresponding blockage ratios are 0:03 and 0:06 respectively. With reference to Figure 3.8, the x - axis is vertical and aligned with the mean flow direction. The z - axis coincides with the cylinder axis and the y - axis is perpendicular to both x and z .

Module 3: Velocity Measurement

Lecture 12: Introduction to PIV

Flow in the test section was set up by a small fan driven by a single phase motor. The suction side of the fan was used to draw the flow from the test cell. The power supply to the blower was from an online uninterrupted power supply unit to ensure practically constant input voltage to the motor.

For better control of the voltage setting, particularly at low fan RPM and hence at low flow rates, the output of the UPS was stepped down via two variacs connected in series. In turn, this had the effect of minimizing the velocity fluctuations in the approach flow. The free stream turbulence level in the approach flow was quite small and it was found to be less than the background noise of the anemometer ($< 0.05\%$). Flow parallelism in the approach flow was better than 98% over 95% of the width of the test cell. The validation of the test cell is discussed in a later section of the present module.



(a)



(b)



(c)

Fig 3.10: PIV components: (a) CCD Camera (b) Nd-YAG laser (c) Synchronizer

Module 3: Velocity Measurement

Lecture 12: Introduction to PIV

The flow to the test cell goes through three parts, namely the settling chamber, a honeycomb section and a contraction cone. Fine screens are mounted in the settling chamber for reducing the turbulence level of flow entering the test section. The contraction ratio of the contraction cone in area units is 10:1.

The contraction cone reduces the spatial irregularities in the velocity distribution and helps in the decay of turbulence intensity by proper stretching of the vortices. The function of the honeycomb is to straighten the flow by damping the transverse components of velocity, and to reduce the turbulence level by suppressing the turbulence scales that are larger than the size of a honeycomb cell. The screens are used to suppress the small disturbances generated at the outlet tips of the honey comb. Proper mesh size gradation has been utilized by examining the diameter of the elements of the honeycomb, and hence the length scale of the vortices generated. Specially, two screens, one with a coarse grid (10 per cm^2) and the other with a fine grid (100 per cm^2) have been used in the test cell.

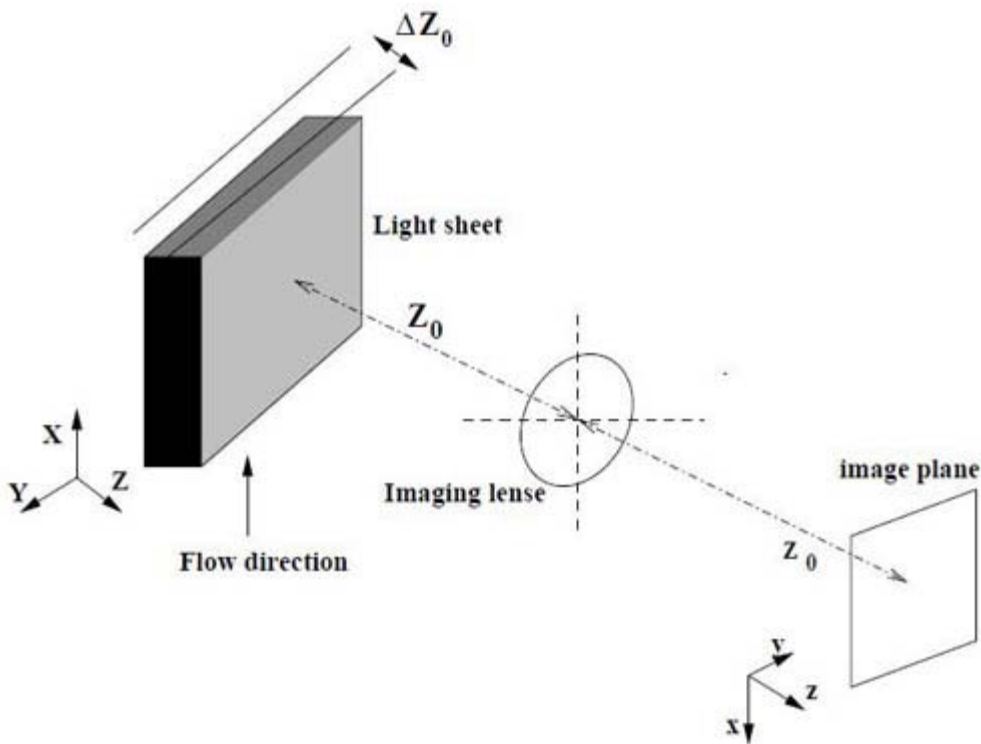


Fig 3.11: Imaging system for PIV

Module 3: Velocity Measurement

Lecture 12: Introduction to PIV

Contd...

The distance maintained between the mesh and honeycomb has been selected by trial and error, to ensure that the smoothest possible flow approaches the square cylinder. Stable velocities in the range of 0.5– 3 m/s could realized in the test section. These values correspond to a Reynolds number range of 100 - 700 for the cylinder sizes referred earlier. A seeding arrangement is fitted prior to the honeycomb for PIV measurements.

 **Previous** **Next** 

Particle Image Velocimetry

Traditionally, quantitative measurements of fluid velocity have been carried out using a pitot-static tube and hotwire anemometry. Both these techniques require insertion of a physical probe into the flow domain. This process is intrusive and can alter the flow field itself. In addition, measurements are averages over a small representative volume. The probe has to be physically displaced to various locations to scan the entire region of interest. The development of cost-effective lasers led to the development of Laser Doppler velocimeter (LDV) that uses a laser probe to enable non-intrusive velocity measurements. Velocity information by LDV however, is obtained point-wise similar to that of the pitot-static tube and the hotwire probe. Particle image velocimetry (PIV) is the state-of-the-art technique for velocity measurement in experimental fluid mechanics. Original contributions towards its development were made by Adrian (1991), Gharib (1991), Melling (1997), and Westerweel (1997). The most important advantage of PIV is that it is a non-intrusive technique and gives the spatial details of the flow field over a plane of interest. There is some flexibility in the choice of the measuring plane. The measurement process can be repeated in time to yield temporal evolution of the flow field. The ability to make global velocity measurements makes PIV a special tool in experimental fluid mechanics. With PIV, it is possible to acquire practically instantaneous velocity fields with high spatial resolution. The spatial resolution is limited by the thickness of the laser sheet and the choice of the interrogation spot during analysis. The latter is about 8 or 16 pixels. The smallest length scale that can be detected depends on the size of the pixel, and hence the spatial resolution of the camera. Depending on the camera speed, a time series of images can be recorded during experiments. The ensemble average of the instantaneous velocity vectors yields the time-averaged velocity field. This includes zones of reversed flow that cannot be dealt with by hotwire and pitot probes. Once the velocity field is obtained, other quantities such as vorticity, strain rates and momentum fluxes can be estimated. With developments in lasers, camera and high speed/low cost computers it is now possible to use PIV regularly for research and industrial applications.



Module 3: Velocity Measurement

Lecture 12: Introduction to PIV

The picture of the PIV setup is shown in Figure 3.9 and the photograph of important hardware of PIV is shown in Figure 3.10. In the present experiments, PIV measurements were carried out at selected planes perpendicular and parallel to the cylinder axis. A double pulsed Nd:YAG laser of wavelength $\lambda = 532\text{nm}$ and 15 mJ/pulse with a maximum repetition rate of 15Hz per laser head was used. The light sheet had a maximum scan area of $10 \times 10\text{ cm}^2$. The sheet thickness was about 1 mm to minimize the effect of the out-of-plane velocity component. The assembly of Peltier-cooled 12 bit CCD camera and frame grabber with a frame speed of 8Hz was used for acquisition of PIV images. Figure 3.11 shows geometric diagram of PIV measurements. A cross section of the flow is illuminated with a thin light sheet, and the tracer particles in the light sheet are projected onto a recording medium (CCD) in the image plane of a lens as shown in Figure 3.11. The intensity of the light sheet thickness ΔZ_0 is assumed to change only in the Z direction. The magnification of particle image depends upon the position of the imaging lens. The CCD consisted of an array of 1280×1024 pixels. A Nikon 50 mm manual lens with $f^\# = 1.4$ was attached to the CCD camera for covering the field of interest. Both the camera and laser were synchronized with a synchronizer controlled by a dual processor PC. The field of view employed in the present set of PIV measurements was 40 mm by 35 mm. Velocity vectors were calculated from particle traces by the adaptive cross-correlation method. The final interrogation size was 16×16 pixels starting from an initial size of 64×64 . Thus, 5561 velocity vectors were obtained in the imaging area with a spatial resolution of 0.5 mm. Inconsistent velocity vectors were eliminated by local median filtering and subsequently replaced by interpolated data from adjacent vectors. The laser pulse width was $20\ \mu\text{s}$ and the time delay between two successive pulses was varied from 40 to $200\ \mu\text{s}$ depending on the fluid velocity (Keane and Adrian, 1990). The time-averaged velocity field was obtained by averaging a sequence of 200 velocity vector images, corresponding to a total time duration of 50 seconds. Laskin nozzles were used to produce seeding particles from corn oil. The mean diameter of oil particles was estimated to be $2\ \mu\text{s}$. Data generated from PIV carries superimposed noise. Noise is introduced during recording of PIV images (optical distortion, light sheet non-homogeneity, transfer function of the CCD, non-spherical particles, and speckle) and during data processing (peak fitting algorithm, image interpolation and peak deformation). The validation of the PIV technique was carried out by comparing velocities with pitot static tube and hotwire anemometry, as discussed in later sections.

◀ Previous Next ▶

Seeding arrangement for PIV

One of the most important steps in PIV measurements is seeding of the flow. In order to consider PIV as a non-intrusive technique, it is necessary that the addition of tracer particle does not alter the flow properties. Proper seeding is essential to capture complicated flow details, for example, the recirculation zone. Seeding should be homogeneous (spatially uniform) and sufficient (of high enough density). The injection of tracer particle has to be done without significantly disturbing the flow, but in a way and at a location that ensures homogeneous distribution of the tracers. Particles should be of small diameter so that they follow the original local air velocity without causing any disturbance. The particle density should ideally match that of the fluid to eliminate velocity lag. This issue is adequately taken care of by micron-sized particles for which surface forces are in excess of body forces.

For the present investigation, tracer particles (namely, droplets of corn oil) were added to the main air flow by a number of copper tubes upstream of the honeycomb section. A large number of tiny holes, 0.1 mm diameter were drilled along the length of the copper tubes to make the seeding uniform over the entire test section. The seeding density was adjusted through an air pressure control valve. Laskin nozzles were used to produce oil droplets as tracers. For the range of frequencies in the wake, an expected slip velocity error of 0.3% to 0.5% relative to the instantaneous local velocity is expected in the present study (Adrian, 1991).

Laskin nozzles are widely used as atomizers of non-volatile liquids due to simplicity of design and the resulting uniform particle size distribution. The picture of the Laskin nozzle seed generator has been shown in [Figure 3.12](#). A detailed schematic drawing of the Laskin nozzle seed generator is shown in [Figure 3.13](#). The particles should be small in size, spherical in shape, of appropriate density and refractive index, and non-volatile. Above all, the liquid should be non-toxic and of low cost. The particles should be efficient scatterer of the illuminating laser light. This largely decides the illuminating laser type and the recording hardware i.e. camera. For example, if a given particle scatters weakly, then one would have to employ more powerful lasers or a more sensitive camera, both of which can drive up costs, as well as the associated safety issues. Corn oil was used for the present work, in view of its high surface tension required for producing small particles along with favorable light scattering properties.



Fig 3.12: Picture of the Laskin nozzle seed generator

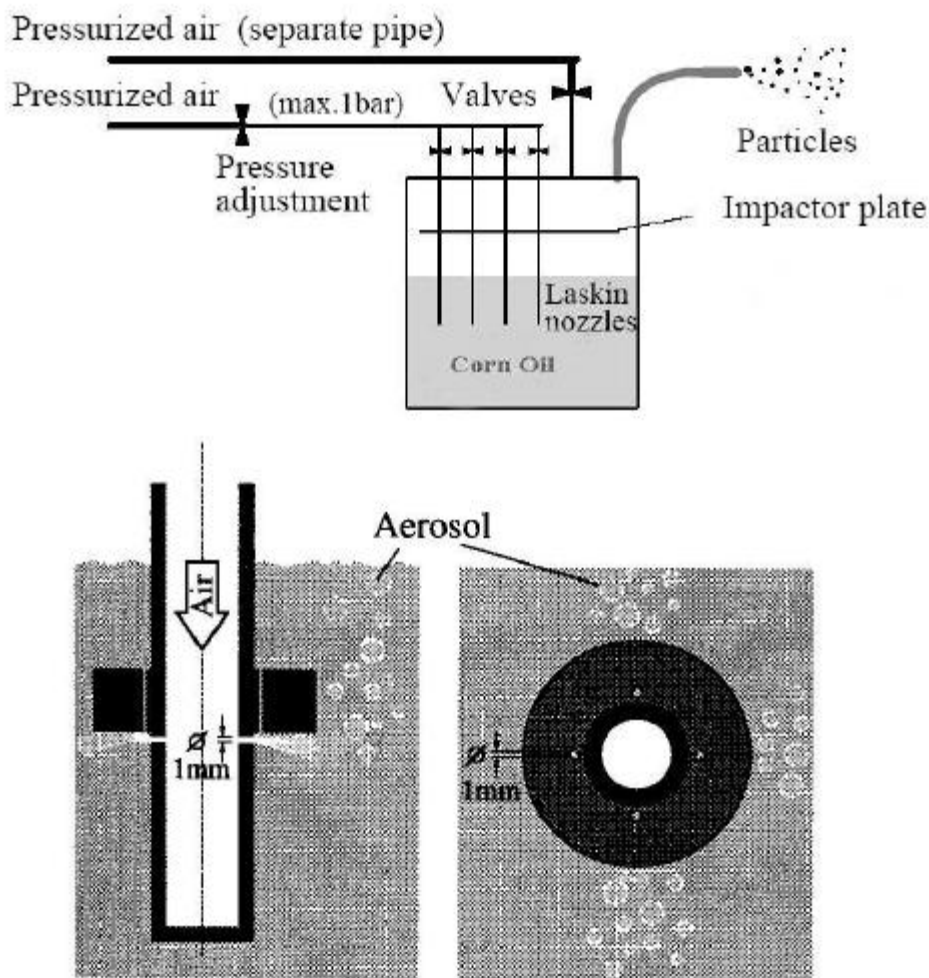


Fig 3.13: Schematic of the Laskin nozzle used for the seeding generation

An important source of error in velocity measurement is the particle weight. The following analysis ascertains that particle weight is not a major consideration in the present experiments in the sense that particles would follow the main flow without excessive slip. The approach is to find the settling velocity of the particles under a gravity field. Assuming that Stokes law of drag is applicable, the settling velocity u_{∞} is given by

$$u_{\infty} = \frac{gd_p^2(\rho_p - \rho_f)}{18\mu}$$

Here d_p and ρ_p are the particle diameter and density respectively, and μ and ρ_f are the fluid viscosity and density respectively. Particles are suitable as long as u_{∞} is negligible compare to actual fluid velocity. For the present set experiments, u_{∞} was estimated to be 0.014 m/s.

Particle Dynamics

The particle dynamics as outlined by Adrian (1991) for successful PIV measurements is discussed in this section. The PIV technique measures in principle the Lagrangian velocities of the particle, \mathbf{v} . If the particle velocity is being used to infer Eulerian fluid velocity $\mathbf{u}(\mathbf{x}, t)$, one must consider the accuracy with which the particle follows the fluid motion. With subscript p denoting particle-level properties, the equation of motion of a single particle in a dilute suspension is a balance between inertia and drag force is written as:

$$\rho_p \frac{\pi d_p^3}{6} \frac{d\mathbf{v}}{dt} = C_D \frac{\rho \pi d_p^2}{4} |\mathbf{v} - \mathbf{u}| (\mathbf{v} - \mathbf{u}) \quad (1)$$

The above equation requires a correction for the added mass of the fluid, unsteady drag forces, pressure gradients in the fluid, and nonuniform fluid motion. In gaseous flows with small liquid particles, we may ignore all these terms except the static drag law with drag coefficient C_D . This term incorporates finite Reynolds number effects.

Particle response is often described in terms of the flow velocity and a characteristic frequency of oscillation. The first question is, how fast can the flow be, before the particle lag $|\mathbf{v} - \mathbf{u}|$ creates an unacceptably large error. An appropriate approach is to evaluate the particle slip velocity as a function of the applied acceleration. For the simplified drag law of the above equation, one has

$$|\mathbf{v} - \mathbf{u}| = \left[\frac{2}{3} \frac{\rho_p}{\rho} \frac{d_p}{C_D} |\dot{\mathbf{v}}| \right]^{\frac{1}{2}} \quad (2)$$

This shows that the slip velocity for finite particle Reynolds number, where $C_D \sim \text{constant}$, is only proportional to the square root of the acceleration. In the limit of small particle Reynolds number $|\mathbf{v} - \mathbf{u}| d_p / \nu \leq 1$, Stokes' law may be used to evaluate C_D resulting in

$$|\mathbf{v} - \mathbf{u}| = \frac{\rho_p d_p^2 |\dot{\mathbf{v}}|}{36 \rho \nu} \quad (3)$$

Module 3: Velocity Measurement

Lecture 12: Introduction to PIV

The time separation Δt is the single most important adjustable variable in a PIV system, as it determines the maximum and minimum velocities that can be measured. The duration of the light pulses δt , determines the degree to which an image is frozen during the pulse exposure. The accuracy of velocity measurements depends upon one's ability to determine the displacement of the particle, Δx over a certain time interval from measurements of the displacement of the image ΔX .

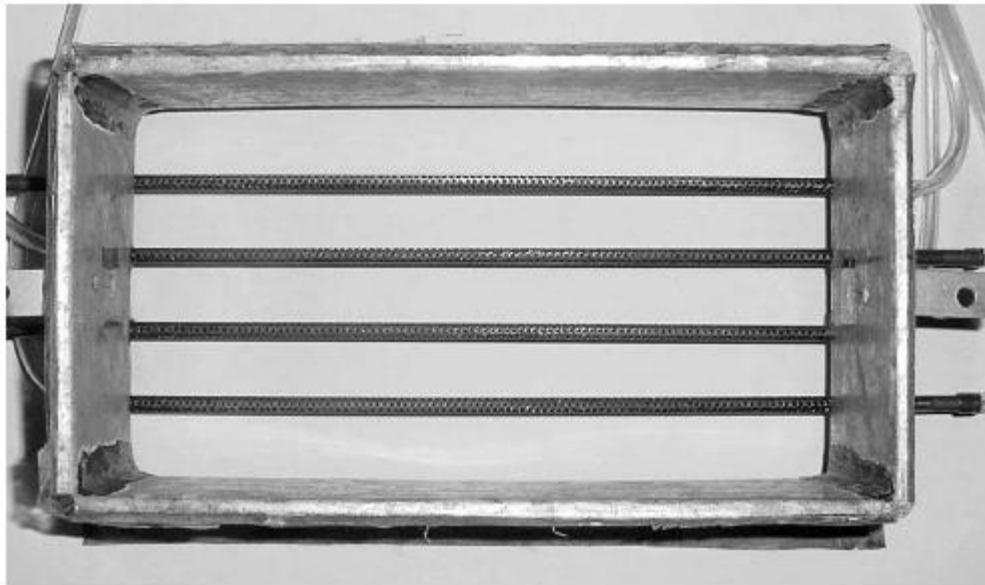


Fig 3.14: Distributed hole arrangement for uniform seeding distribution.

Generating a light sheet

For PIV measurement a high intensity light source is required for efficient scattering of light from tracer particles. Light sheet is generated from a collimating laser beam using cylindrical lens and spherical lens. The effective intensity of a light sheet can be increased by sweeping a light beam to form sheet thereby concentrating the energy by a factor equal to the height of the light sheet divided by the height of the beam. Figure 3.15 shows the schematic of a light sheet formation. A combination of cylindrical and spherical lens is used. A negative focal length lens is first used to avoid focal line. The cylindrical lens causes the laser beam to expand in one direction only, i.e. it "fans" the beam out. The position of the minimum thickness is determined by the focal length of the cylindrical lens. The spherical lens causes the expanding beam to focus along the perpendicular direction, at a distance of one focal length downstream to the beam waist.

Synchronizer

In order to make PIV measurements, different components of the PIV system need to be time coordinated, for example, the camera, the laser flash lamps and its Q-switches. The synchronizer controls the time sequence. A part of the functions is executed automatically, while others have to be defined by the user. The synchronizer thus manages all the timing events needed for doing PIV measurements.

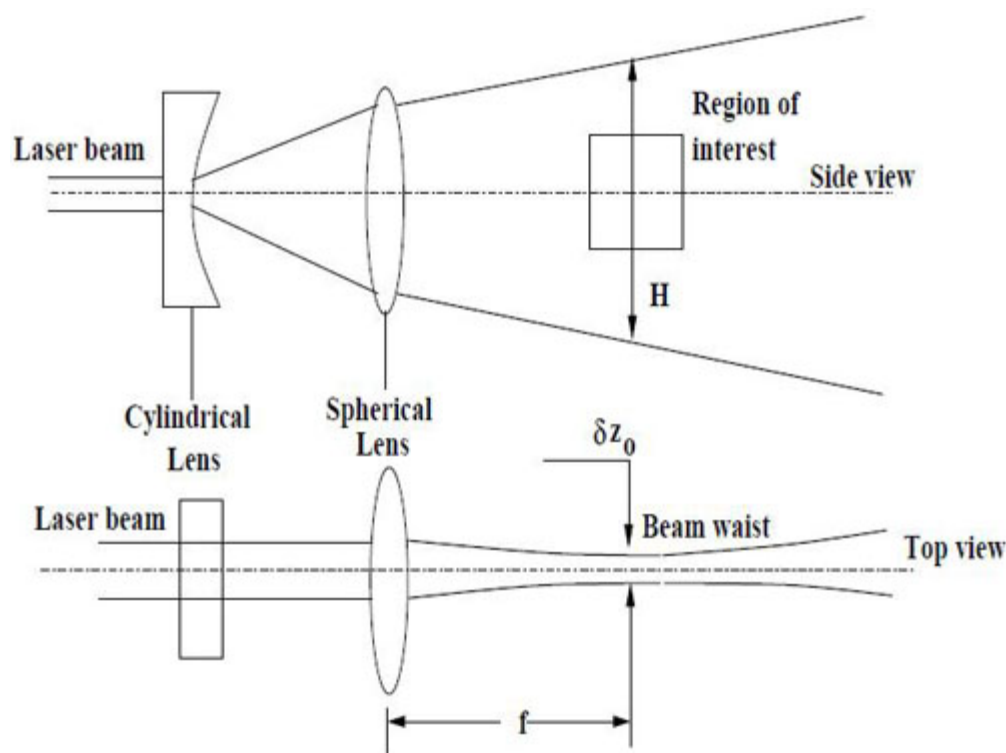


Fig 3.15: Light sheet formation using spherical and cylindrical lens for PIV.

Module 3: Velocity Measurement

Lecture 12: Introduction to PIV

The frame grabber needs 40 ns to lock onto the trigger signal. Afterwards, the control data can be transferred to the camera. The exposure time is controlled by the external trigger from the synchronizer in a user-defined range between 100 ns and 1 ms. Before the second exposure, the camera has a frame straddling time of 200 ns or 1 μs which depends on the parameter settings of the cross correlation function. Before the next double exposure can be started, data of the first image pair is transferred to the frame grabber.

The laser must be synchronized to the double exposure mode of the camera. For emitting a laser pulse, a high energy must be generated in the laser cavity. The laser cavity has a Nd:YAG rod that is pumped with energy from a flash lamp. There is a nonlinear relation between the time the cavity is pumped and laser power emitted. During the pumping procedure, the mirror at the far end of the cavity is closed by a Q-switch. The success of PIV measurements depends crucially on the time correlation between laser pulse generation and camera recording achieved by the synchronizer unit. Figure 3.16 shows the timing diagram for the pulsed laser with double shutter CCD camera.

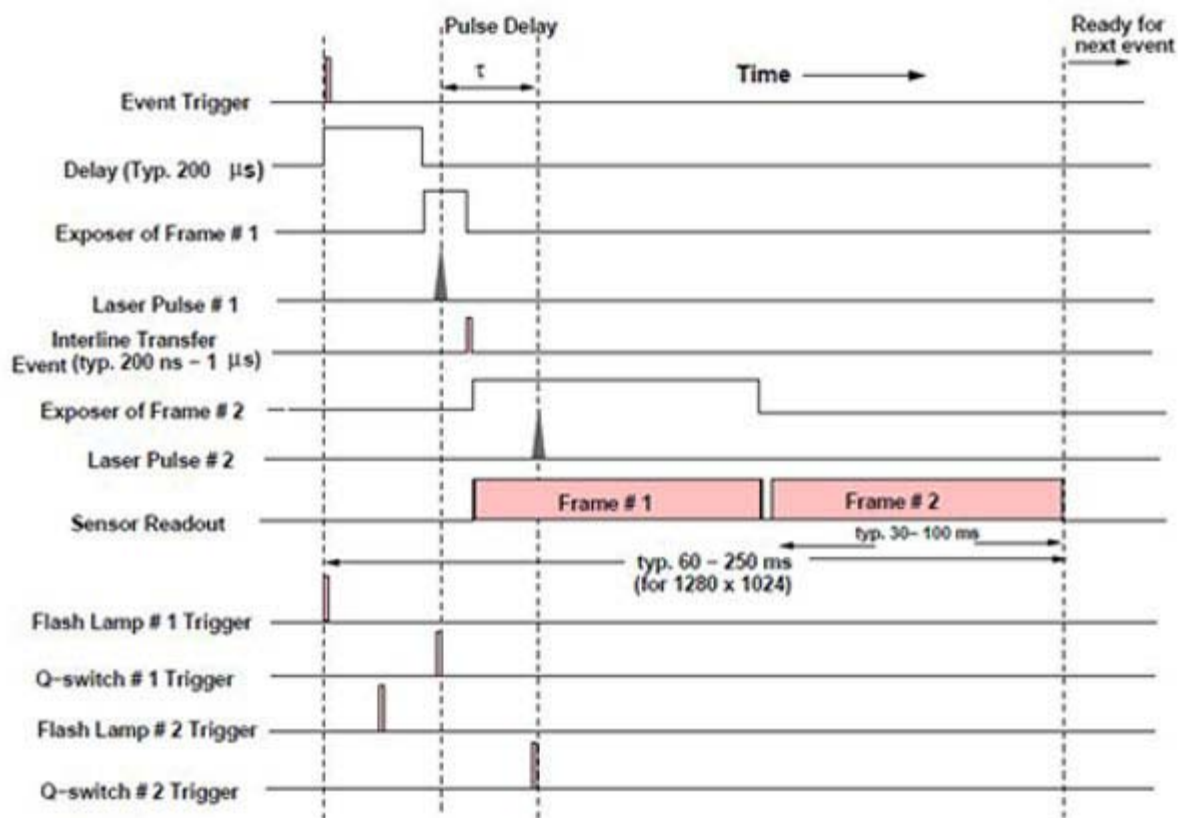


Fig 3.16: Timing diagram for CCD camera and double pulsed laser (PIV Manual, Oxford Lasers).